 cmes, vol.6, no.1, pp.43-58, 2004

2.5D Green's Functions in the Frequency Domain for Heat Conduction Problems in Unbounded, Half-space, Slab and Layered Media

António Tadeu[1], **Julieta António and Nuno Simões**

Abstract: This Analytical Green's functions for the steady-state response of homogeneous three-dimensional unbounded, half-space, slab and layered solid media subjected to a spatially sinusoidal harmonic heat line source are presented. In the literature, this problem is frequently referred to as the two-and-a-half dimensional fundamental solution or 2.5D Green's functions.

The proposed equations are theoretically interesting in themselves and they are also useful as benchmark results for validating numerical applications. They are also of great practical use in the formulation of three-dimensional heat transfer problems in layered solid formations using integral transform methods and/or boundary elements.

The final expressions for heat conduction in an unbounded medium are validated first, since time solutions are known in analytical form. This requires the prior application of an inverse Fourier transform to our frequency domain results, using complex frequencies to avoid the aliasing phenomena. The results provided by the proposed expressions for half-space and slab are then compared with those computed using the image source technique, while the solutions obtained for the layered media are then verified with those calculated by the Boundary Element Method solution, which requires the discretization of the interfaces between layers with boundary elements.

keyword: Green's functions, transient heat conduction, frequency domain

1 Introduction

The most important reference for heat transfer is Carslaw and Jaeger's book (1959), which contains a set of analytical solutions and Green's functions for the diffusion equation. It also includes an extensive survey of numerical methods, which can be grouped according to how the time-dependent terms are dealt with. The first is a "time marching" approach in which the solution is evaluated step by step at successive time intervals after an initially specified state has been defined. The second uses the Laplace transform of the time in which the diffusion equation becomes an elliptical one. After the solution has been obtained for a sequence of values of the transform parameter, a numerical transform inversion is used to compute the physical variables in the real space.

Although the Laplace transform has been widely used for solving diffusion problems, accuracy depends on an efficient and precise inverse transform, since small truncation errors can be magnified in the inversion process. Several inversion methods have been proposed over the years, such as the Stehfest algorithm (1970).

The present work provides Green's functions for computing the heat radiated by a spatially sinusoidal, harmonic heat line source placed in solid formations with varying configurations: unbounded, half-space, slab and layered media. These expressions, or fundamental solutions, relate the heat field variables (fluxes or temperatures) at some location in the solid domain caused by a heat source placed elsewhere in the media.

This type of heat source can be seen as resulting from applying a time Fourier transform to the heat point source and then a spatial Fourier transform in the direction in which the geometry does not vary (z). The 3D heat field in the time domain can be then synthesized by using the inverse Fourier transforms in the frequency and wavenumber (k_z) domain. If we assume the existence of virtual heat sources equally spaced, Lz, along z, this inverse Fourier transformation becomes a discrete summation, which allows the solution to be obtained by solving a limited number of two-dimensional problems. The time-aliasing phenomenon can be avoided by using complex frequencies to attenuate the response at the end of

[1] Department of Civil Engineering,
Faculty of Sciences and Technology
University of Coimbra, Portugal

the time frame. This effect is later taken into account by re-scaling the response in the time domain.

Thus, the Green's functions for the case of a spatially sinusoidal, harmonic heat line source placed in an unbounded medium are developed by first applying a time Fourier transform to the time diffusion equation for a heat point source and then a spatial Fourier transform to the resulting Helmholtz equation, along the z direction, in the frequency domain.

The derivation of the Green's functions for the layered solid formations requires expressing the Green's function for the unbounded media as a superposition of heat generated by plane diffusion sources. This follows the approach similar to the one used first by Lamb (1904) for the propagation of elastodynamic waves in a two-dimensional media, and then by other authors such as Bouchon (1979) and Tadeu and António (2001) to compute three-dimensional elastodynamic fields using a discrete wave number representation. In other elastodynamic related work Luco and De Barros (1995) computed the three-dimensional seismic response of a layered cylindrical valley. Zhang and Chopra (1991) used the direct boundary element to compute the impedance matrix for a three-dimensional foundation supported on an infinitely long canyon of uniform cross-section cut in a homogenous half space. Stamos and Beskos (1996) calculated the 3D dynamic response of long, lined tunnels of uniform cross-section in a half-space subjected to a plane harmonic waves propagating in an arbitrary direction using the BEM formulation. Notice that the search for Green's functions has been object of research over the years because these expressions can be used as benchmark solutions, which can be incorporated in the development of numerical methods such as the Boundary Elements Method (see, for example, Kögl and Gaul (2000), Manolis and Pavlou (2002)Ochiai (2001), Sellountos and Polyzos (2003)and Zhang and Savaidis(2003)).

In this work the heat conduction Green's functions for a half space and a slab can be expressed as the sum of the heat source terms equal to those in the full-space and the surface terms required to satisfy the boundary conditions at the surfaces, which can be of two types: null normal fluxes or null temperatures. A similar technique is used to find the Green's functions for a layered formation. The final heat field is computed as the sum of the heat source terms equal to those in the full-space and a set of surface terms, generated within each solid layer and at each interface. The amplitudes of these surface terms are defined after ascribing the required boundary conditions: continuity of temperatures and normal fluxes between solid layers, and null normal fluxes or null temperatures at the outer surface.

The expressions presented here make it possible to compute the heat field inside a layered solid medium, without fully discretizing the interior domain, which is required by numerical techniques, such as the finite differences, or even by discretizing the free surface using boundary elements techniques.

The authors believe that the fundamental solutions presented here can be of great value in formulating 3D transient heat conduction problems via boundary elements together with integral transforms, in layered media such as composite laminated slabs, building walls and ground building floors. The fundamental solutions are expressed in an explicit form, and represent the Green's functions for a harmonic (steady-state) line heat source load placed in an unbounded, half-space, slab and layered medium, whose amplitude varies sinusoidally in the third dimension. Such problems are referred to in the literature as 2.5D problems. These equations are very important in themselves, they can both relate the temperatures and heat fluxes at some point produced by a point load somewhere in the three-dimensional space, and be incorporated into a numerical boundary element approach designed to avoid the full discretization of the solid layered interfaces. Notice that this full discretization is only possible using various simplified approaches, such as damping, otherwise it will lead to a system of equations that is too large to be solved.

This paper first formulates the three-dimensional problem and explains how the Green's functions for a sinusoidal heat line source, applied in an unbounded solid formation, can be obtained and written as a continuous superposition of plane waves in the frequency domain. A brief description of how the time solutions are obtained is also given. In order to validate our solutions, the results obtained for one, two and three-dimensional heat sources in an unbounded medium are compared with those provided by analytical expressions, known in the time domain.

Then, a similar procedure is applied to the Green's functions for a sinusoidal line pressure load applied to a half space and a slab with differing boundary conditions. In these cases, the image model technique can be also used

to define these Green's functions and this is thus used to validate the solutions. This technique employs virtual heat sources (image heat sources) to compute the heat field. These heat sources are placed so that they can simulate the reflections caused by the boundaries.

Finally, the Green's functions for a layered solid formation are established using the required boundary conditions at the various interfaces. The full set of expressions is compared with those provided by the Boundary Element Method (BEM), for which a full discretization of the boundary interfaces is required.

2 3D problem formulation and Green's Functions in an Unbounded Medium

The solution of transient heat conduction in solids is described by the diffusion equation

$$\nabla^2 T = \frac{1}{K}\frac{\partial T}{\partial t} \tag{1}$$

where $\nabla^2 = \left(\frac{\partial^2}{\partial x^2} + \frac{\partial^2}{\partial y^2} + \frac{\partial^2}{\partial z^2}\right)$, t is time, $T(t,x,y,z)$ is temperature, $K = \frac{k}{\rho\, c}$ is the thermal diffusivity, k is the thermal conductivity, ρ is the density and c is the specific heat. Applying a Fourier transform in the time domain, one obtains

$$\left(\nabla^2 + \left(\sqrt{\frac{-\mathrm{i}\omega}{K}}\right)^2\right)\hat{T}(\omega,x,y,z) = 0 \tag{2}$$

where $\mathrm{i} = \sqrt{-1}$ and ω is the frequency. Equation (2) is a Helmholtz equation similar to the one used to solve acoustic problems, where $\omega/(velocity\,of\,pressure\,waves)$ corresponds to $\sqrt{\frac{-\mathrm{i}\omega}{K}}$ in the diffusion equation. Thus, the transient heat propagation solution can be seen as an harmonic propagation of heat.

The fundamental solution of equation (2) for a heat point source in an unbounded medium, located at $(x_0, y_0, 0)$, $p(\omega,x,y,z,t) = \delta(x-x_0)\,\delta(y-y_0)\,\delta(z)\,e^{\mathrm{i}(\omega t)}$ where $\delta(x-x_0)$, $\delta(y-y_0)$ and $\delta(z)$ are Dirac-delta functions, can be written as

$$\hat{T}_f(\omega,x,y,z) = \frac{1}{2k\sqrt{(x-x_0)^2+(y-y_0)^2+z^2}}\, e^{-\sqrt{\frac{\mathrm{i}\omega}{K}}\sqrt{(x-x_0)^2+(y-y_0)^2+z^2}} \tag{3}$$

In many cases, the analysis of 3D problems can become computationally demanding, and it is often best to express the full 3D problem as a summation of simpler 2D solutions, when the geometry of the problem remains constant along one direction (z). This is achieved by applying a Fourier transformation along that direction, and expressing the solution as a summation of 2D solutions, with different spatial wavenumbers k_z (Tadeu and Kausel (2000)). The application of a spatial Fourier transformation along the z direction to the equation (2) leads to the following equation

$$\left(\tilde{\nabla}^2 + \left(\sqrt{\frac{-\mathrm{i}\omega}{K} - (k_z)^2}\right)^2\right)\tilde{T}(\omega,x,y,k_z) = 0 \tag{4}$$

with $\tilde{\nabla}^2 = \left(\frac{\partial^2}{\partial x^2} + \frac{\partial^2}{\partial y^2}\right)$.

Applying a spatial Fourier transform, in the z direction, to the fundamental equation for a heat point source (equation (3)) gives the fundamental solution for this equation,

$$\tilde{T}_f(\omega,x,y,k_z) = \frac{-\mathrm{i}}{4k} H_0\left(\sqrt{\frac{-i\omega}{K} - (k_z)^2}\, r_0\right) \tag{5}$$

where $H_n()$ are Hankel functions of the second kind and order n, and $r_0 = \sqrt{(x-x_0)^2+(y-y_0)^2}$. This response can be seen as the response to a spatially varying heat line source of the form $p(\omega,x,y,k_z,t) = \delta(x-x_0)\,\delta(y-y_0)\,e^{\mathrm{i}(\omega t - k_z z)}$ (see Fig. 1).

The full three-dimensional solution is then obtained by applying an inverse Fourier transform along the k_z domain. If we assume the existence of virtual sources equally spaced, L_z, along z, this inverse Fourier transformation becomes a discrete summation, which allows the solution to be obtained by solving a limited number of two-dimensional problems.

$$\hat{T}(\omega,x,y,z) = \frac{2\pi}{L}\sum_{m=-M}^{M}\tilde{T}(\omega,x,y,k_{zm})\,e^{-\mathrm{i}k_{zm}z} \tag{6}$$

with k_{zm} being the axial wavenumber given by $k_{zm} = \frac{2\pi}{L_z}m$. The distance L_z must be sufficiently large to avoid spatial contamination from the virtual sources [Bouchon and Aki (1977)]. A similar procedure has been used by the authors to analyze the wave propagation inside seismic prospecting boreholes [Tadeu et al. (2002)] and the

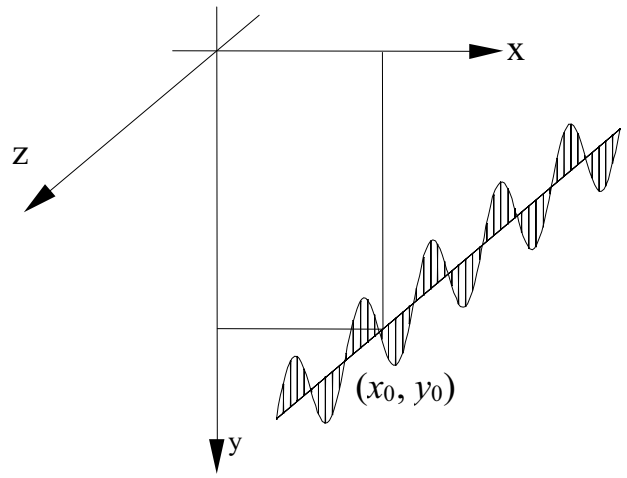

Figure 1 : Spatially harmonic varying line load

outdoor propagation of sound waves in the presence of obstacles [Godinho et al. (2001)].

These same equations can be expressed as a continuous superposition of heat generated by plane diffusion sources. Equation (5), which results from a spatially sinusoidal harmonic heat line source along the *z* direction, applied at the point (x_0, y_0), is then given by the expressions,

$$\tilde{T}_f(\omega, x, y, k_z) = \frac{-\mathrm{i}}{4\pi k} \int_{-\infty}^{+\infty} \left(\frac{e^{-\mathrm{i}\nu|y-y_0|}}{\nu} \right) e^{-\mathrm{i}k_x(x-x_0)} dk_x \quad (7)$$

where $\nu = \sqrt{\frac{-\mathrm{i}\omega}{K} - k_z^2 - k_x^2}$ with $(Im(\nu) \leq 0)$, and the integration is performed with respect to the horizontal wave number (k_x) along the *x* direction.

The transformation of this integral into a summation can be achieved if an infinite number of such sources are distributed along the *x* direction, at equal intervals L_x. The above equation can then be written as

$$\tilde{T}_f(\omega, x, y, k_z) = E_0 \sum_{n=-\infty}^{n=+\infty} \left(\frac{E}{\nu_n} \right) E_d \quad (8)$$

where $E_0 = \frac{-\mathrm{i}}{2kL_x}$

$E = e^{-\mathrm{i}\nu_n|y-y_0|}$

$E_d = e^{-\mathrm{i}k_{xn}(x-x_0)}$

$\nu_n = \sqrt{\frac{-\mathrm{i}\omega}{K} - k_z^2 - k_{xn}^2}$ with $(Im(\nu_n) \leq 0)$

$k_{xn} = \frac{2\pi}{L_x} n$

which can in turn be approximated by a finite sum of equations (N).

Notice that $k_z = 0$ corresponds to the two-dimensional case.

2.1 Responses in the time domain

The heat in the spatial-temporal domain is obtained by a numerical inverse fast Fourier transform in k_z and the frequency domain. Complex frequencies with a small imaginary part of the form $\omega_c = \omega - \mathrm{i}\eta$ (with $\eta = 0.7\Delta\omega$, being $\Delta\omega$ the frequency step) are used to avoid the aliasing phenomena. In the time domain, this shift is later taken into account by applying an exponential window of the form $e^{\eta t}$ to the response.

The temporal variation of the source can be arbitrary. The application of a time Fourier transformation defines the frequency domain where the BEM solution is required. So the frequency domain may range from 0.0 Hz to very high frequencies. However, we may cut off the upper frequencies of this domain because the heat responses decrease very fast as the frequency increases. The frequency 0.0 Hz is the static response that can be obtained by limiting the frequency to zero. As we are using complex frequencies, the response can be computed because the argument of the Hankel function in equation (5) is $-\mathrm{i}\eta$, that is, other than zero.

As stated before, the Fourier transformations are achieved by discrete summations over wavenumbers and frequencies, a procedure which is mathematically equivalent to adding periodic sources at spatial intervals $L_z = 2\pi/\Delta k_z$ (in the z-axis), and temporal intervals $T = 2\pi/\Delta\omega$, with Δk_z being the wavenumber step. The spatial separation L_z must be such that contamination of the response by the periodic sources cannot occur. In other words, the contribution to the response by the fictitious sources must be guaranteed to occur at times later than T. Achievement of this goal can also be aided substantially by the shift adopted for the frequency axis $(\omega_c = \omega - \mathrm{i}\eta)$. This technique results in the significant attenuation or virtual elimination of the periodic sources.

2.2 Responses in the time domain

The procedures described in the previous section were implemented and validated by using them to calculate the one, two and three dimensional exact time solutions for a unit heat source placed in an unbounded medium. The exact solution of the diffusion equation (1) in an unbounded medium in the time domain, describing the temperature field generated by a unit heat source applied at point (x_0, y_0, z_0) at time $t = t_0$, is

$$T(t,x,y,z) = \frac{1}{\rho c\,(4\pi k\tau)^{d/2}} e^{\left(-\frac{r_{00}^2}{4k\tau}\right)} \quad \text{if } t > t_0 \tag{9}$$

where $\tau = t - t_0$, r_{00} is the distance between the source point and the field point (x,y,z), and $d = 3$, $d = 2$ and $d = 1$ when in the presence of a three, two and one-dimensional problem, respectively (Carslaw and Jaeger (1959)).

Consider a homogeneous unbounded solid medium with thermal material properties that allow $k = 1.4\,\mathrm{W.m^{-1}.^oC^{-1}}$, $c = 880.0\,\mathrm{J.Kg^{-1}.^oC^{-1}}$ and $\rho = 2300\,\mathrm{Kg.m^{-3}}$. At time $t = 277.8\,\mathrm{h}$, a unit heat source is excited at ($x = 0.0\,\mathrm{m}, y = 0.0\,\mathrm{m}$, $z = 0.0\,\mathrm{m}$). Figure 3 displays the temperature computed using equation (9), along a line of 40 receivers placed from $y = -1.5\,\mathrm{m}$ to $y = 1.5\,\mathrm{m}$, (see Fig. 2) for a plane ($d = 1$), cylindrical ($d = 2$) and spherical ($d = 3$) unit heat source, at different times.

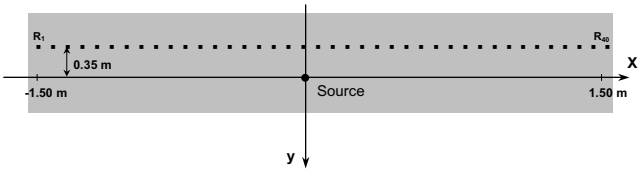

Figure 2 : Geometry of the problem

The heat responses at these receivers were also computed using the proposed Green's function. Computations are performed in the frequency range [0,1024$x10^{-7}$ Hz] with a frequency increment of $\Delta\omega = 10^{-7}\,\mathrm{Hz}$, which defines a time window of $T = 2777.8\,\mathrm{h}$. The solution for a plane unit heat source propagating along the y axis has been modeled ascribing $k_z = 0$ and $k_{xn} = 0$ to equation (8) multiplied by L_x.

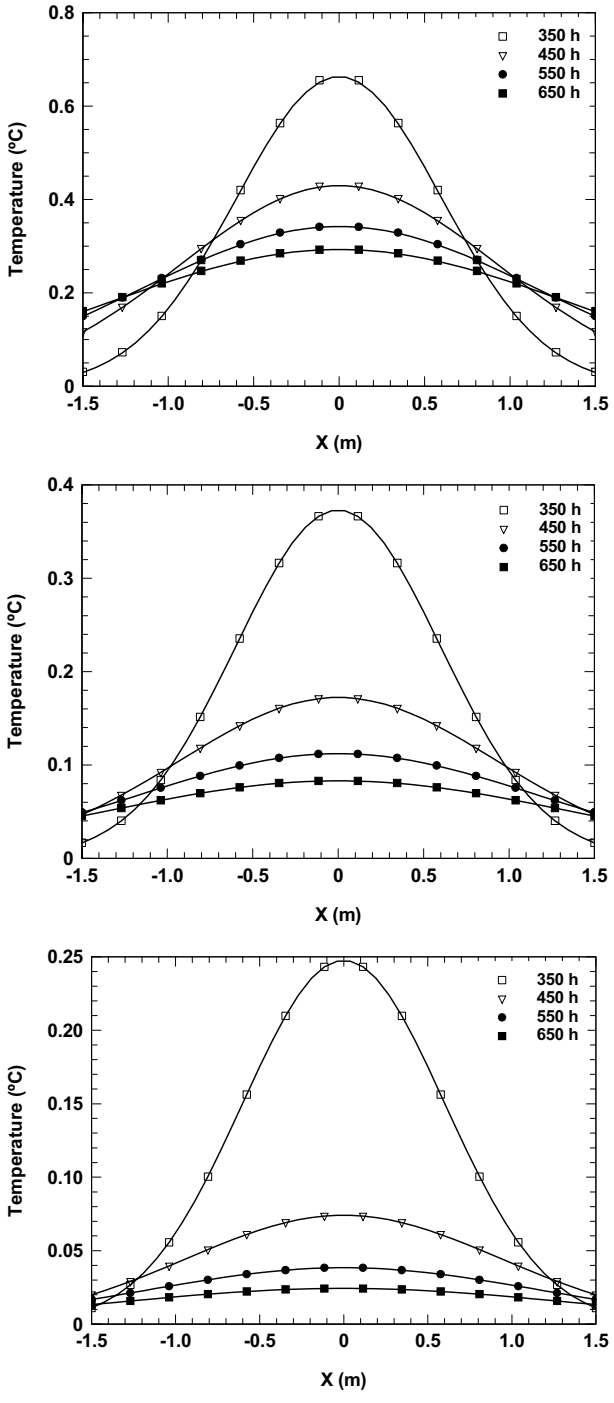

Figure 3 : Temperature along a line of 40 receivers, at different times (350 h, 450 h, 550 h and 650 h): a) for a plane ($d = 1$) unit heat source; b) for a cylindrical ($d = 2$) unit heat source; c) for a spherical ($d = 3$) unit heat source

The solution for a cylindrical unit heat source has been calculated using equation (5), ascribing $k_z = 0$, while the response for a spherical unit heat source has been obtained using equation (3) divided by 2π. Complex frequencies of the form $\omega_c = \omega - 0.7i\Delta\omega$ have been used to avoid the aliasing phenomenon. The markers in Fig. 3 display the response computed using the proposed Green's functions, and the solid line represents the solution given by equation (9). The agreement between these two solutions is excellent.

The cylindrical and the spherical unit heat source responses have also been computed performing discrete summations over wavenumbers, following equations (6) and (8), which is mathematically equivalent to adding sources at spatial intervals L_x, L_z. The spatial period has been set as $L_x = L_z = 2\sqrt{k/(\rho\, c\, \Delta f)}$. The agreement among solutions has also proved to be excellent.

3 Green's Functions in a Half-space

The Green's functions for a half-space solid formation can be expressed as the sum of the source terms equal to those in the full-space and the surface terms needed to satisfy the free-surface conditions (null heat fluxes or null temperatures). These surface terms can be expressed in a form similar to that of the source term, namely,

$$\tilde{T}_1(\omega,x,y,k_z) = E_0 \sum_{n=-\infty}^{n=+\infty} \left(\frac{E_a}{\nu_n} A_n\right) E_d \tag{10}$$

where $E_a = e^{-i\nu_n y}$. A_n is as yet unknown coefficient to be determined from the appropriate boundary conditions, so that the field produced simultaneously by the source and surface terms should produce $\tilde{T}_1(\omega,x,y,k_z) = 0$ or $\frac{\partial \tilde{T}_1(\omega,x,y,k_z)}{\partial y} = 0$ at $y = 0$.

The imposition of the stated boundary conditions for each value of *n* leads to an equation in the one unknown constant. The final result will then be obtained,

Null normal flux at $y = 0$,

$$A_n = e^{-i\nu_n y_0}$$

Null temperature at $y = 0$,

$$A_n = -e^{-i\nu_n y_0} \tag{11}$$

Having obtained the constant, we may compute the heat associated with the surface terms by means of equation (10).

Null normal flux at $y = 0$,

$$\tilde{T}_1(\omega,x,y,k_z) = E_0 \sum_{n=-\infty}^{n=+\infty} \left(\frac{E_{af}}{\nu_n}\right) E_d$$

Null temperature at $y = 0$,

$$\tilde{T}_1(\omega,x,y,k_z) = E_0 \sum_{n=-\infty}^{n=+\infty} \left(\frac{E_{at}}{\nu_n}\right) E_d \tag{12}$$

where $E_{af} = e^{-i\nu_n(y+y_0)}$ and $E_{at} = -e^{-i\nu_n(y+y_0)}$.

The Green's functions for a half-space are then given by the sum of the source terms and these surface terms. After adding these terms together, we get expressions for the half-space of the form:

Null normal flux at $y = 0$,

$$\tilde{T}(\omega,x,y,k_z) = E_0 \sum_{n=-\infty}^{n=+\infty} \left(\frac{E + E_{af}}{\nu_n}\right) E_d \tag{13}$$

Null temperature at $y = 0$,

$$\tilde{T}(\omega,x,y,k_z) = E_0 \sum_{n=-\infty}^{n=+\infty} \left(\frac{E - E_{at}}{\nu_n}\right) E_d \tag{14}$$

which can be written as

Null normal flux at $y = 0$,

$$\tilde{T}(\omega,x,y,k_z) = \frac{-i}{4k}\left[H_0(K_t r_0) + H_0(K_t r_1)\right] \tag{15}$$

Null temperature at $y = 0$,

$$\tilde{T}(\omega,x,y,k_z) = \frac{-i}{4k}\left[H_0(K_t r_0) - H_0(K_t r_1)\right] \tag{16}$$

where $r_1 = \sqrt{(x-x_0)^2 + (y+y_0)^2}$ and $K_t = \sqrt{\frac{-i\omega}{K} - (k_z)^2}$.

3.1 Validation of the Solution

The image model technique employs virtual sources (image sources) to compute the heat field. These sources are placed so that they can simulate the reflections caused by the reflecting boundaries. This technique is reliable, but

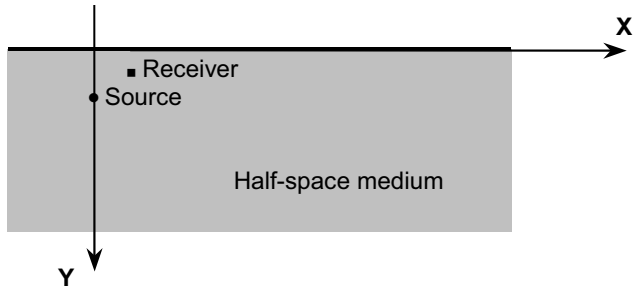

Figure 4 : Geometry of the problem for a half-space formation

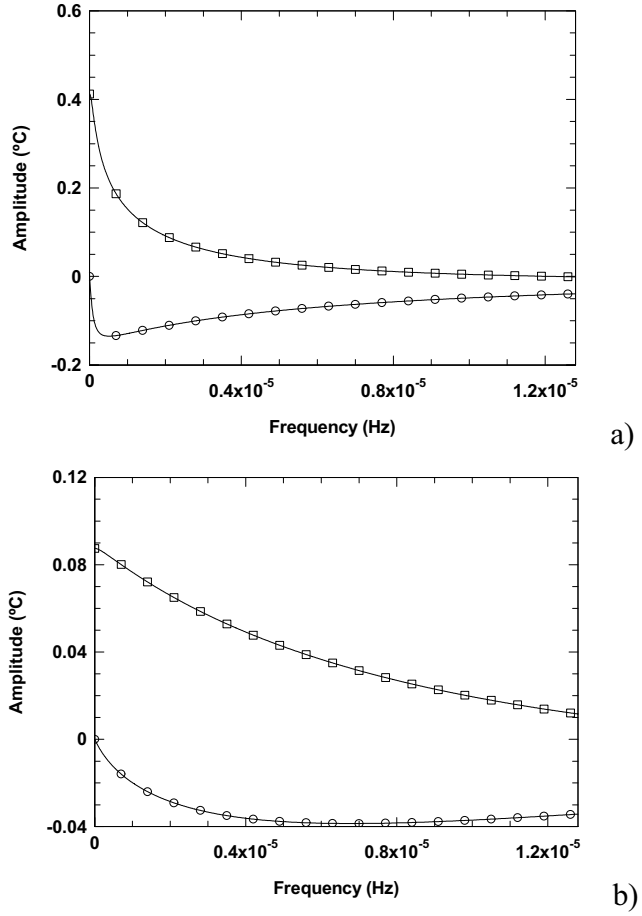

Figure 5 : Real and imaginary parts of the response for a half-space solid formation with spatial wavenumber $k_z = 0.4$ rad / m: a) Null normal flux at $y = 0$. b) Null temperature at $y = 0$

the computations involving models with complex geometry can become very complicated, and entail high computational costs. In this simpler case we may find that the image model technique will yield the same results as those given by equation (13). Notice that the position of the virtual source required to solve the present problem would be placed at $(x_0, -y_0)$.

Figure 5 presents the results obtained at the receiver $(x = 0.1\,\mathrm{m}, y = 0.1\,\mathrm{m})$ when a line heat source with spatial sinusoidal variation ($k_z = 0.4$ rad / m) is excited at $(x = 0.0\,\mathrm{m}, y = 0.2\,\mathrm{m})$ in a homogeneous solid half-space medium with thermal material properties that allow $k = 1.4\,\mathrm{W.m^{-1}.^oC^{-1}}$, $c = 880.0\,\mathrm{J.Kg^{-1}.^oC^{-1}}$ and $\rho = 2300\,\mathrm{Kg.m^{-3}}$ (see Fig. 4). The solid line represents the results provided by the proposed solutions while the markers correspond to the solution computed using the image source technique. The square and the round marks indicate the real and imaginary part of the responses, respectively. The results allow verifying that both solutions are similar.

4 Green's functions in a solid slab formation

The Green's functions for a solid slab formation with thickness h can be expressed as the sum of the source terms equal to those in the full-space and the surface terms needed to satisfy the boundary conditions at the two slab surfaces (null heat fluxes or null temperatures). Both interfaces (top and bottom) generate surface terms which can be expressed in a form similar to that of the source term,

Solid medium (top surface)

$$\tilde{T}_1(\omega, x, y, k_z) = E_0 \sum_{n=-\infty}^{n=+\infty} \left(\frac{E_a}{\nu_n} A_n^t \right) E_d$$

Solid medium (bottom surface)

$$\tilde{T}_2(\omega, x, y, k_z) = E_0 \sum_{n=-\infty}^{n=+\infty} \left(\frac{E_b}{\nu_n} A_n^b \right) E_d \qquad (17)$$

where, $E_b = e^{-i\nu_n |y-h|}$. A_n^t and A_n^b are as yet unknown coefficients to be defined by imposing the appropriate boundary conditions, so that the field produced simultaneously by the source and the surface terms guarantees null heat fluxes or null temperatures at $y = 0$ and at $y = h$.

The imposition of the two stated boundary conditions for each value of n leads to a system of two equations in

the two unknown constants. Three different cases are defined in terms of null heat fluxes or null temperatures prescribed for the top and bottom surfaces.

Case I - null heat fluxes at the top and bottom surfaces.

$$\begin{bmatrix} 1 & -e^{-\mathrm{i}\nu_n h} \\ e^{-\mathrm{i}\nu_n h} & -1 \end{bmatrix} \begin{bmatrix} A_n^t \\ A_n^b \end{bmatrix} = \begin{bmatrix} e^{-\mathrm{i}\nu_n y_0} \\ -e^{-\mathrm{i}\nu_n |h-y_0|} \end{bmatrix} \tag{18}$$

Case II - null temperatures at the top surface and null heat fluxes at the bottom surface.

$$\begin{bmatrix} 1 & e^{-\mathrm{i}\nu_n h} \\ e^{-\mathrm{i}\nu_n h} & -1 \end{bmatrix} \begin{bmatrix} A_n^t \\ A_n^b \end{bmatrix} = \begin{bmatrix} -e^{-\mathrm{i}\nu_n y_0} \\ -e^{-\mathrm{i}\nu_n |h-y_0|} \end{bmatrix} \tag{19}$$

Case III - null temperatures at the top and bottom surfaces.

$$\begin{bmatrix} 1 & -e^{-\mathrm{i}\nu_n h} \\ e^{-\mathrm{i}\nu_n h} & 1 \end{bmatrix} \begin{bmatrix} A_n^t \\ A_n^b \end{bmatrix} = \begin{bmatrix} -e^{-\mathrm{i}\nu_n y_0} \\ -e^{-\mathrm{i}\nu_n |h-y_0|} \end{bmatrix} \tag{20}$$

Once this system of equations has been solved, the amplitude of the surface terms has been fully defined, and the heat propagation in the slab can thus be found. The final expressions for the Green's functions are then derived from the sum of the source terms and the surface terms originated in the two free surfaces, which leads to the following expressions,

$$\tilde{T}(\omega, x, y, k_z) = \frac{-\mathrm{i}}{4k} H_0(K_t\, r_0) + E_0 \sum_{n=-\infty}^{n=+\infty} \left(\frac{E_a}{\nu_n} A_n^t + \frac{E_b}{\nu_n} A_n^b \right) E_d \tag{21}$$

4.1 Validation of the Solution

The expressions described above were used to calculate the heat field generated by a spatially harmonic varying line load in the z direction, in a slab 0.5 m thick. The results provided were then compared with those arrived at by using the image model function that can be derived for the present case.

This function can be achieved by superposing the heat field generated by virtual sources with positive or negative polarity, and located so that the desired boundary conditions are ensured.

Case I - null heat fluxes at the top and bottom surfaces.

$$\tilde{T}(\omega, x, y, k_z) = \frac{-\mathrm{i}}{4k} [H_0(K_t r_0)] + \frac{-\mathrm{i}}{4k} \left\{ \sum_{m=0}^{NS} \left[\sum_{j=1}^{4} H_0(K_t r_j) \right] \right\} \tag{22}$$

Case II - null temperatures at the top surface and null heat fluxes at the bottom surface.

$$\tilde{T}(\omega, x, y, k_z) = \frac{-\mathrm{i}}{4k} [H_0(K_t r_0)] + \frac{-\mathrm{i}}{4k} \left\{ \sum_{m=0}^{NS} (-1)^m [-H_0(K_t r_1) + H_0(K_t r_2) - H_0(K_t r_3) - H_0(K_t r_4)] \right\} \tag{23}$$

Case III - null temperatures at the top and bottom surfaces.

$$\tilde{T}(\omega, x, y, k_z) = \frac{-\mathrm{i}}{4k} [H_0(K_t r_0)] + \frac{-\mathrm{i}}{4k} \left\{ \sum_{m=0}^{NS} [-H_0(K_t r_1) - H_0(K_t r_2) + H_0(K_t r_3) + H_0(K_t r_4)] \right\} \tag{24}$$

in which

$$r_1 = \sqrt{(x-x_0)^2 + (y+y_0+2hm)^2}$$

$$r_2 = \sqrt{(x-x_0)^2 + (y-2h+y_0-2hm)^2}$$

$$r_3 = \sqrt{(x-x_0)^2 + (y+2h-y_0+2hm)^2}$$

$$r_4 = \sqrt{(x-x_0)^2 + (y-2h-y_0-2hm)^2}$$

The number of sources to be used (NS) is determined so that all the signals needed to define the signal within the time interval fixed by the frequency increment are taken into account.

For the three scenarios above, the medium remains constant, so that $k = 1.4\,\mathrm{W.m^{-1}.^oC^{-1}}$, $c = 880.0\,\mathrm{J.Kg^{-1}.^oC^{-1}}$ and $\rho = 2300.0\,\mathrm{Kg.m^{-3}}$. The slab

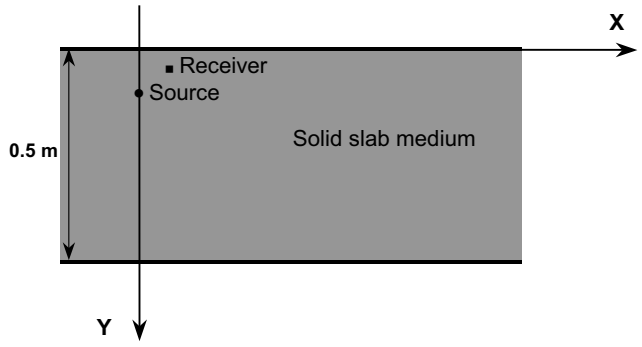

Figure 6 : Geometry of the problem for a solid slab formation

is heated by a harmonic point heat source applied at the point $(x = 0.0\,\mathrm{m}, y = 0.2\,\mathrm{m})$ (see Fig. 6).

Calculations are performed in the frequency range $[0, 128x10^{-7}\,\mathrm{Hz}]$ with a frequency increment of $\Delta\omega = 10^{-7}\,\mathrm{Hz}$. The imaginary part of the frequency has been set to $\eta = 0.7\Delta\omega$. To validate the results, the response is computed at a single value of $k_z (k_z = 0.4\,\mathrm{rad/m})$. The real and imaginary parts of the responses at the receiver $(x = 0.1\,\mathrm{m}, y = 0.1\,\mathrm{m})$ are shown in Fig. 7. The solid lines represent the discrete analytical responses, while the marked points correspond to the image model technique. The square and the round marks indicate the real and imaginary part of the responses, respectively. As can be seen, these two solutions are in very close agreement, and equally good results were obtained from tests in which heat sources and receivers were situated at different points.

5 Green's functions in a layered formation

Next, the Green's functions for a solid layer over a solid half-space, a solid layer bounded by two semi infinite solid media and a multi-solid layer are established using the required boundary conditions at the solid-solid interfaces and at the free surface.

5.1 Solid layer over a solid half-space

The solution is again expressed as the sum of the source terms (the incident field) equal to those in the full-space and the surface terms needed to satisfy the continuity of temperature and normal fluxes at the solid-solid interface and null heat fluxes or null temperatures at the top surface (see Fig. 8). All solid interfaces $(1, 2)$ generate surface

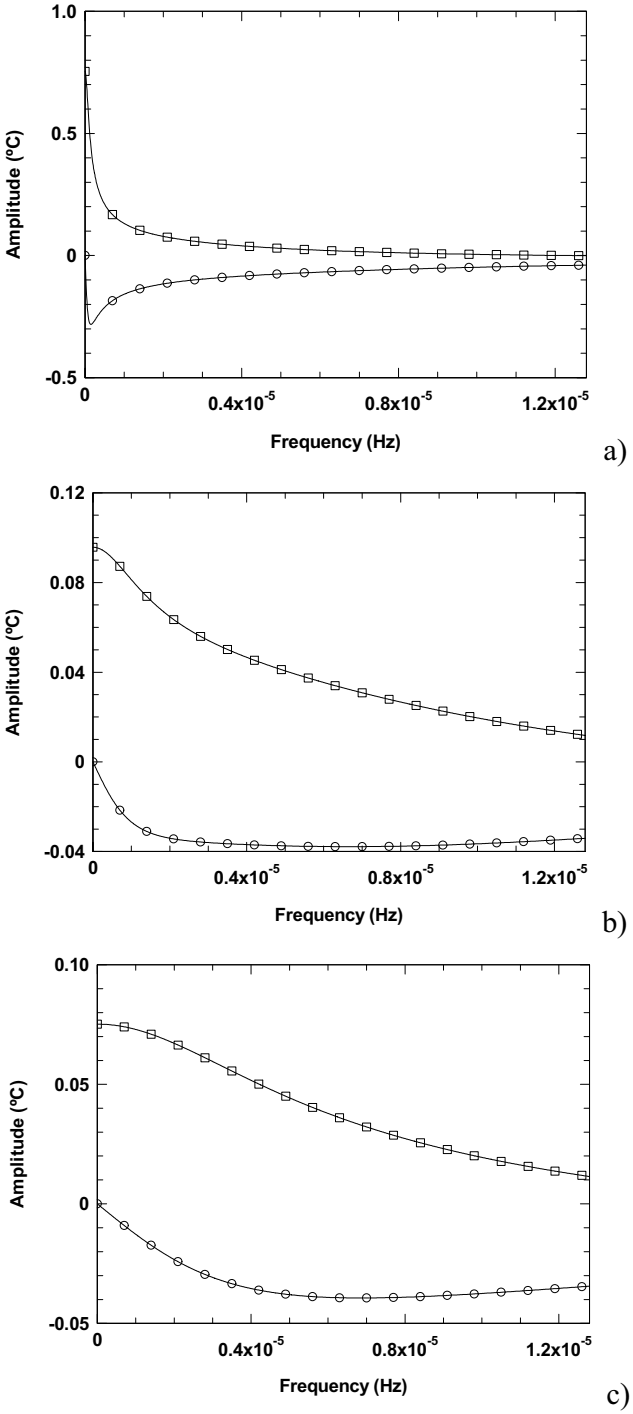

Figure 7 : Real and imaginary parts of the responses for a solid slab formation. Heat source applied at the point $(x = 0.0\,\mathrm{m}, y = 0.2\,\mathrm{m})$: a) Case I (null heat fluxes at the top and bottom surfaces). b) Case II (null temperatures at the top surface and null heat fluxes at the bottom surface). c) Case III (null temperatures at the top and bottom surfaces). Heat source applied at the point $(x = 0.0\,\mathrm{m}, y = 0.2\,\mathrm{m})$

terms, which can be expressed in a form similar to that of the source term.

Solid layer (interface 1)

$$\tilde{T}_{11}(\omega,x,y,k_z) = E_{01}\sum_{n=-\infty}^{n=+\infty}\left(\frac{E_{11}}{\nu_{n1}}A_{n1}^{t}\right)E_d \tag{25}$$

Solid layer (interface 2)

$$\tilde{T}_{12}(\omega,x,y,k_z) = E_{01}\sum_{n=-\infty}^{n=+\infty}\left(\frac{E_{12}}{\nu_{n1}}A_{n1}^{b}\right)E_d \tag{26}$$

Half space (interface 2)

$$\tilde{T}_{21}(\omega,x,y,k_z) = E_{02}\sum_{n=-\infty}^{n=+\infty}\left(\frac{E_{21}}{\nu_{n2}}A_{n2}^{t}\right)E_d \tag{27}$$

where $E_{0j} = \frac{-\mathrm{i}}{2k_jL_x}$, $E_{11} = e^{-\mathrm{i}\nu_{n1}y}$, $E_{12} = e^{-i\nu_{n1}|y-h_1|}$, $E_{21} = e^{-\mathrm{i}\nu_{n2}|y-h_1|}$, $\nu_{nj} = \sqrt{\frac{-\mathrm{i}\omega}{K_j} - k_z^2 - k_{xn}^2}$ with $Im(\nu_{nj}) \leq 0$ and h_1 is the layer thickness ($j=1$ stands for the solid layer (medium 1) while $j=2$ indicates the solid half-space (medium 2)). Meanwhile, $K_j = \frac{k_j}{\rho_j c_j}$ is the thermal diffusivity in the solid medium j (k_j, ρ_j and c_j are the thermal conductivity, the density and the specific heat of the material in the solid medium j, respectively).

The coefficients A_{n1}^t, A_{n1}^b and A_{n2}^t are as yet unknown coefficients to be obtained from the appropriate boundary conditions, so that the field produced simultaneously by the source and surface terms leads to the continuity of heat fluxes and temperatures at $y = h_1$, and null heat fluxes (Case I) or null temperatures (Case II) at $y = 0$.

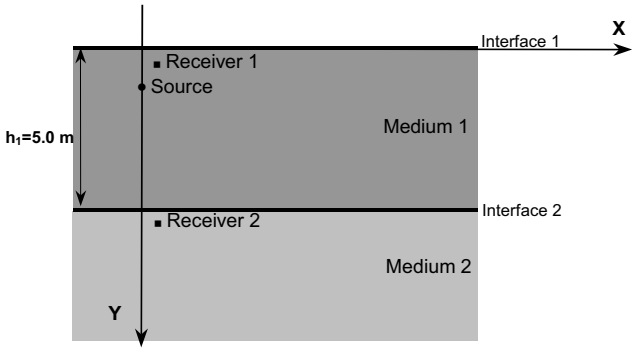

Figure 8 : Geometry of the problem for a solid layer over a solid half-space

Imposing the three stated boundary conditions for each value of n, a system of three equations in the three unknown coefficients is defined.

Case I - null heat fluxes at $y = 0$.

$$\begin{bmatrix} 1 & -e^{-\mathrm{i}\nu_{n1}h_1} & 0 \\ e^{-\mathrm{i}\nu_{n1}h_1} & -1 & -1 \\ e^{-\mathrm{i}\nu_{n1}h_1} & 1 & -\frac{k_1\nu_{n1}}{k_2\nu_{n2}} \end{bmatrix}\begin{bmatrix} A_{n1}^t \\ A_{n1}^b \\ A_{n2}^t \end{bmatrix} = \begin{bmatrix} b_1 \\ b_2 \\ b_3 \end{bmatrix} \tag{28}$$

where

$b_1 = e^{-\mathrm{i}\nu_{n1}y_0}$

$b_2 = -e^{-\mathrm{i}\nu_{n1}|h_1-y_0|}$

$b_3 = -e^{-\mathrm{i}\nu_{n1}|h_1-y_0|}$

when the source is in the solid layer ($y_0 < h_1$),

while

$b_1 = 0$

$b_2 = -e^{-\mathrm{i}\nu_{n2}|h_1-y_0|}$

$b_3 = \frac{k_1\nu_{n1}}{k_2\nu_{n2}}e^{-\mathrm{i}\nu_{n2}|h_1-y_0|}$

when the source is in the half-space ($y_0 > h_1$).

Case II - null temperatures at $y = 0$.

$$\begin{bmatrix} 1 & e^{-\mathrm{i}\nu_{n1}h_1} & 0 \\ e^{-\mathrm{i}\nu_{n1}h_1} & -1 & -1 \\ e^{-\mathrm{i}\nu_{n1}h_1} & 1 & -\frac{k_1\nu_{n1}}{k_2\nu_{n2}} \end{bmatrix}\begin{bmatrix} A_{n1}^t \\ A_{n1}^b \\ A_{n2}^t \end{bmatrix} = \begin{bmatrix} b_1 \\ b_2 \\ b_3 \end{bmatrix} \tag{29}$$

where

$b_1 = -e^{-\mathrm{i}\nu_{n1}y_0}$

$b_2 = -e^{-\mathrm{i}\nu_{n1}|h_1-y_0|}$

$b_3 = -e^{-\mathrm{i}\nu_{n1}|h_1-y_0|}$when the source is in the solid layer ($y_0 < h_1$),

while

$b_1 = 0$

$b_2 = -e^{-\mathrm{i}\nu_{n2}|h_1-y_0|}$

$b_3 = \frac{k_1\nu_{n1}}{k_2\nu_{n2}}e^{-\mathrm{i}\nu_{n2}|h_1-y_0|}$when the source is in the half-space ($y_0 > h_1$).

The heat within the two solid media is then computed by adding the contributions of the source terms to those associated with the surface terms generated at the various interfaces.

$$y_0 < h_1$$

$$\tilde{T}(\omega,x,y,k_z) = \frac{-\mathrm{i}}{4k_1} H_0(K_{t1}\, r_0) +$$

$$E_{01} \sum_{n=-\infty}^{n=+\infty} \left(\frac{E_{11}}{\nu_{n1}} A^t_{n1} + \frac{E_{12}}{\nu_{n1}} A^b_{n1} \right) E_d \quad \text{if } y < h_1$$

$$\tilde{T}(\omega,x,y,k_z) = E_{02} \sum_{n=-\infty}^{n=+\infty} \left(\frac{E_{21}}{\nu_{n2}} A^t_{n2} \right) E_d \text{ if } y > h_1 \qquad (30)$$

$$y_0 > h_1$$

$$\tilde{T}(\omega,x,y,k_z) = E_{01} \sum_{n=-\infty}^{n=+\infty} \left(\frac{E_{11}}{\nu_{n1}} A^t_{n1} + \frac{E_{12}}{\nu_{n1}} A^b_{n1} \right) E_d$$

$$\text{if} \quad y < h_1$$

$$\tilde{T}(\omega,x,y,k_z) = \frac{-\mathrm{i}}{4k_2} H_0(K_{t2}\, r_0) +$$

$$E_{02} \sum_{n=-\infty}^{n=+\infty} \left(\frac{E_{21}}{\nu_{n2}} A^t_{n2} \right) E_d \qquad \text{if } y > h_1 \qquad (31)$$

with $K_{tj} = \sqrt{\frac{-\mathrm{i}\omega}{K_j} - (k_z)^2}$ $(j = 1,\, 2)$.

5.2 *Solid layer bounded by two semi-infinite solid media*

In this case, the solution needs additionally to account for the surface heat waves generated in the solid interface 1 which propagate through the top semi-infinite space (medium 0) (see Fig. 9).

$$\tilde{T}_{02}(\omega,x,y,k_z) = E_{00} \sum_{n=-\infty}^{n=+\infty} \left(\frac{E_{01}}{\nu_{n0}} A^b_{n0} \right) E_d \qquad (32)$$

where $E_{0j} = \frac{-\mathrm{i}}{2k_j L_x}$ and $E_{00} = e^{-\mathrm{i}\nu_{n0} y}$.

The surface heat waves, generated in the solid interfaces 1 and 2 and propagating in the solid layer and in bottom semi-infinite space, are expressed as in equations (25-27).

The coefficients A^b_{n0}, A^t_{n1}, A^b_{n1} and A^t_{n2} are computed by imposing the continuity of heat fluxes and temperatures at $y = h_1$ and $y = 0$. This leads to the following system

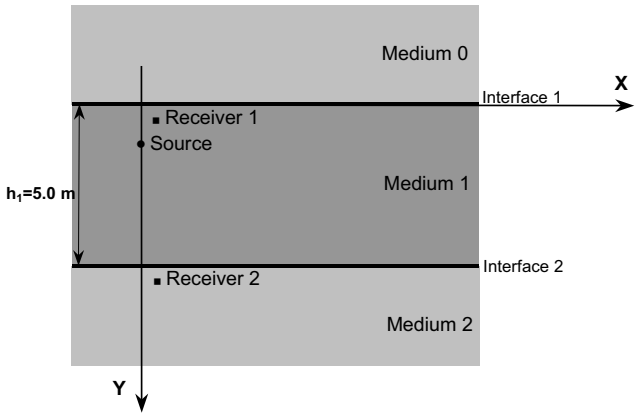

Figure 9 : Geometry of the problem for a solid layer bounded by two semi-infinite solid media

of four equations when the heat source is placed within the solid layer.

$$\begin{bmatrix} -1 & -1 & e^{-\mathrm{i}\nu_{n1}h_1} & 0 \\ \frac{1}{k_0\nu_{n0}} & -\frac{1}{k_1\nu_{n1}} & -\frac{e^{\mathrm{i}\nu_{n1}h_1}}{k_1\nu_{n1}} & 0 \\ 0 & e^{-\mathrm{i}\nu_{n1}h_1} & -1 & -1 \\ 0 & \frac{1}{k_1\nu_{n1}} e^{-\mathrm{i}\nu_{n1}h_1} & \frac{1}{k_1\nu_{n1}} & \frac{1}{k_2\nu_{n2}} \end{bmatrix} \begin{bmatrix} A^b_{n0} \\ A^t_{n1} \\ A^b_{n1} \\ A^t_{n2} \end{bmatrix}$$

$$= \begin{bmatrix} -e^{-\mathrm{i}\nu_{n1}y_0} \\ \frac{1}{k_1\nu_{n1}} e^{-\mathrm{i}\nu_{n1}y_0} \\ -e^{-\mathrm{i}\nu_{n1}|h_1-y_0|} \\ -\frac{1}{k_1\nu_{n1}} e^{-\mathrm{i}\nu_{n1}|h_1-y_0|} \end{bmatrix} \qquad (33)$$

The temperature for the three solid media are then computed by adding the contribution of the source terms to those associated with the surface terms originated at the various interfaces. This procedure produces the following expressions for the temperatures in the three solid media.

$$\tilde{T}(\omega,x,y,k_z) = E_{00} \sum_{n=-\infty}^{n=+\infty} \left(\frac{E_{01}}{\nu_{n0}} A^b_{n0} \right) E_d \quad \text{if } y < 0$$

$$\tilde{T}(\omega,x,y,k_z) = \frac{-\mathrm{i}}{4k_1} H_0(K_{t1}\, r_0)$$

$$+ E_{01} \sum_{n=-\infty}^{n=+\infty} \left(\frac{E_{11}}{\nu_{n1}} A^t_{n1} + \frac{E_{12}}{\nu_{n1}} A^b_{n1} \right) E_d \quad \text{if } 0 < y < h_1$$

$$\tilde{T}(\omega,x,y,k_z) = E_{02} \sum_{n=-\infty}^{n=+\infty} \left(\frac{E_{21}}{\nu_{n2}} A^t_{n2} \right) E_d \quad \text{if } y > h_1 \qquad (34)$$

$$\begin{bmatrix} -1 & -1 & e^{-\mathrm{i}\nu_{n1}h_1} & \dots & 0 & 0 & 0 \\ \frac{1}{k_0\nu_{n0}} & -\frac{1}{k_1\nu_{n1}} & -\frac{e\mathrm{i}}{k_1\nu_{n1}} & \dots & 0 & 0 & 0 \\ 0 & e^{-\mathrm{i}\nu_{n1}h_1} & -1 & \dots & 0 & 0 & 0 \\ 0 & \frac{e^{-\mathrm{i}\nu_{n1}h_1}}{k_1\nu_{n1}} & \frac{1}{k_1\nu_{n1}} & \dots & 0 & 0 & 0 \\ \dots & \dots & \dots & \dots & \dots & \dots & \dots \\ 0 & 0 & 0 & \dots & -1 & e^{-\mathrm{i}\nu_{nm}h_m} & 0 \\ 0 & 0 & 0 & \dots & -\frac{1}{k_1\nu_{nm}} & -\frac{e^{\mathrm{i}\nu_{nm}h_m}}{k_m\nu_{nm}} & 0 \\ 0 & 0 & 0 & \dots & e^{-\mathrm{i}\nu_{nm}h_{m1}} & -1 & -1 \\ 0 & 0 & 0 & \dots & \frac{e^{-\mathrm{i}\nu_{nm}h_m}}{k_m\nu_{nm}} & \frac{1}{k_m\nu_{nm}} & \frac{1}{k_{m+1}\nu_{n(m+1)}} \end{bmatrix} \begin{bmatrix} A^b_{n0} \\ A^t_{n1} \\ A^b_{n1} \\ \dots \\ A^t_{nm} \\ A^b_{nm} \\ A^t_{n(m+1)} \end{bmatrix} = \begin{bmatrix} -e^{-\mathrm{i}\nu_{n1}y_0} \\ \frac{e^{-\mathrm{i}\nu_{n1}y_0}}{k_1\nu_{n1}} \\ -e^{-\mathrm{i}\nu_{n1}\lvert h_1-y_0\rvert} \\ -\frac{e^{-\mathrm{i}\nu_{n1}\lvert h_1-y_0\rvert}}{k_1\nu_{n1}} \\ \dots \\ 0 \\ 0 \\ 0 \\ 0 \end{bmatrix} \tag{37}$$

The derivation presented assumed that the spatially sinusoidal harmonic heat source is placed within the solid layer. However, the equations can be easily manipulated to accommodate another position of the source.

5.3 Multi-solid layer

Consider a medium built from a set of m solid flat layers of infinite extent bounded by flat, semi-infinite, solid media (top semi-infinite medium (medium 0) and bottom semi-infinite medium (medium $m+1$)). The thermal material properties and thicknesses of the different layers may differ. This system is excited by a spatially sinusoidal heat source placed in the first layer (medium 1). The solution is obtained by adapting and extending the models described above. As before, the solution is obtained by adding the direct contribution of the heat source and the surface heat terms generated at all interfaces.

For the solid layer j, the heat surface terms on the upper and lower interfaces can be expressed as

$$\tilde{T}_{j1}(\omega,x,y,k_z) = E_{0j}\sum_{n=-\infty}^{n=+\infty}\left(\frac{E_{j1}}{\nu_{nj}}A^t_{nj}\right)E_d$$

$$\tilde{T}_{j2}(\omega,x,y,k_z) = E_{0j}\sum_{n=-\infty}^{n=+\infty}\left(\frac{E_{j2}}{\nu_{nj}}A^b_{nj}\right)E_d \tag{35}$$

where $E_{j1} = e^{-\mathrm{i}\nu_{n\,j}\left|y-\sum_{l=1}^{j-1}h_l\right|}$, $E_{j2} = e^{-\mathrm{i}\nu_{n\,j}\left|y-\sum_{l=1}^{j}h_l\right|}$ and h_l is the thickness of the layer l. Meanwhile, the heat surface terms generated at interfaces 1 and $m+1$, governing the heat that propagates through the top and bottom semi-infinite media, are respectively expressed by

$$\tilde{T}_{02}(\omega,x,y,k_z) = E_{00}\sum_{n=-\infty}^{n=+\infty}\left(\frac{E_{01}}{\nu_{n0}}A^b_{n0}\right)E_d$$

$$\tilde{T}_{(m+1)2}(\omega,x,y,k_z) = E_{0(m+1)}\sum_{n=-\infty}^{n=+\infty}\left(\frac{E_{(m+1)2}}{\nu_{n(m+1)}}A^t_{n(m+1)}\right)E_d \tag{36}$$

The final system matrix assembled accounts for the coupling between the different layers, so that the heat produced simultaneously by the source and surface terms leads to the continuity of fluxes and temperatures along the $m+1$ solid interfaces. For each value of n, a system of $2(m+1)$ equations in the $2(m+1)$ unknown coefficients is defined ($\underline{\underline{F}}\,\underline{a} = \underline{b}$). (See Equation 37)

Once the amplitude of the surface terms in each solid interface has been obtained, the Green's functions for a solid formation are given by the sum of the source terms and these surface terms, yielding the following expressions,

top semi-infinite medium (medium 0)

$$\tilde{T}(\omega,x,y,k_z) = E_{00}\sum_{n=-\infty}^{n=+\infty}\left(\frac{E_{01}}{\nu_{n0}}A^b_{n0}\right)E_d \quad \text{if } y<0$$

solid layer 1 (source position)

$$\tilde{T}(\omega,x,y,k_z) = \frac{-\mathrm{i}}{4k_1}H_0(K_{t1}\,r_0) + E_{01}\sum_{n=-\infty}^{n=+\infty}\left(\frac{E_{11}}{\nu_{n1}}A^t_{n1} + \frac{E_{12}}{\nu_{n1}}A^b_{n1}\right)E_d \quad \text{if } 0<y<h_1$$

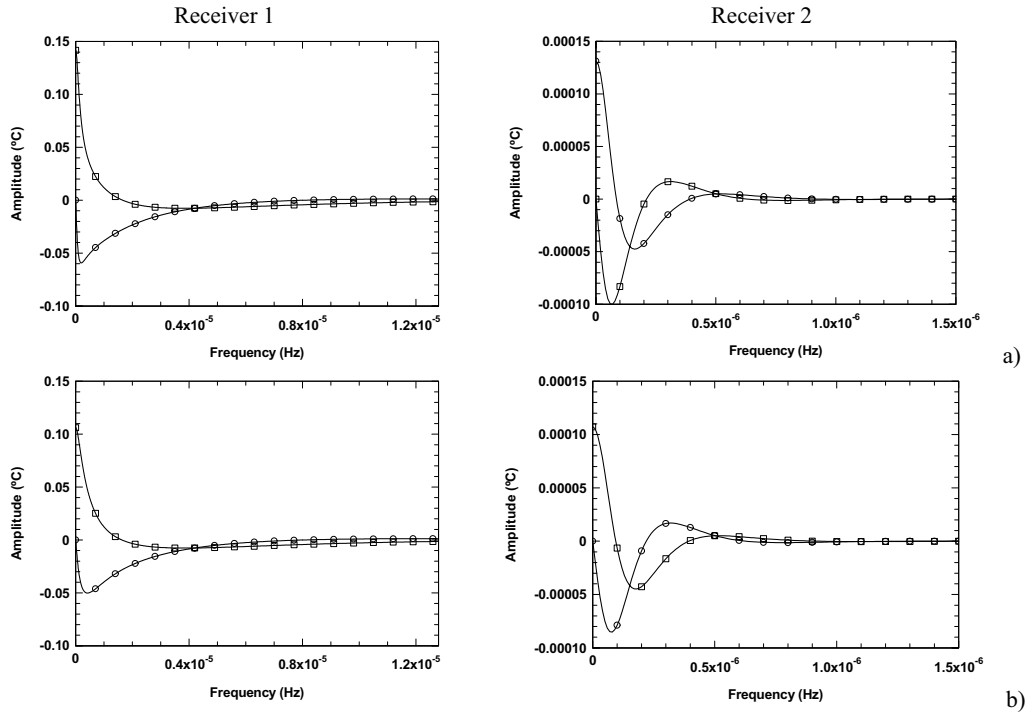

Figure 10 : Solid layer over a solid half-space: a) Case I – null heat fluxes at $y = 0$, responses at receivers 1 and 2. b) Case II – null temperatures at $y = 0$, responses at receivers 1 and 2

solid layer j $(j \neq 1)$

$$\tilde{T}(\omega,x,y,k_z) = E_{0j} \sum_{n=-\infty}^{n=+\infty} \left(\frac{E_{j1}}{\nu_{nj}} A^t_{nj} + \frac{E_{j2}}{\nu_{nj}} A^b_{nj} \right) E_d \quad \text{if}$$

$$\sum_{l=1}^{j-1} h_l < y < \sum_{l=1}^{j} h_l$$

bottom semi-infinite medium (medium $m+1$*)*

$$\tilde{T}_{(m+1)2}(\omega,x,y,k_z) = E_{0(m+1)} \sum_{n=-\infty}^{n=+\infty} \left(\frac{E_{(m+1)2}}{\nu_{n(m+1)}} A^t_{n(m+1)} \right) E_d \tag{38}$$

The solution for a heat source located in a different solid layer can be obtained, maintaining the same matrix system ($\underline{\underline{F}}$) and changing only the independent terms defined by the direct incident field ($\underline{b}$). Thus, the derivation of the total system of equations is quite straightforward, and for this reason is not presented here.

5.4 Validation of the Solution

The results provided by the analytical expressions presented here were compared with those arrived at by applying the BEM model, which requires the discretization of all solid interfaces using the Green's functions for a full space. The BEM code has been validated for the case of circular ring inclusions, for which analytical solutions have already been derived (not included here).

The unlimited discretization of the solid interfaces was avoided by using complex frequencies with a small imaginary part of the form $\omega_c = \omega - i\eta$ (with $\eta = 0.7\Delta\omega$) [Bouchon and Aki (1977), Phinney (1965)]. Boundary elements make a significant contribution to the response up to a definite distance and in the presence of a certain value of damping, but are otherwise unnecessary. These elements are distributed along the surface up to a specific spatial distance. We have computed this distance as $L_{dist} = 2\sqrt{k_j/(\rho_j\, c_j \Delta f)}$. The thermal material properties used were those from the solid medium that leads to the largest spatial distance.

Next, the results are found for the three scenarios. First, a solid flat layer, 5.0 m thick, is assumed to be bounded by one solid half-space. Null heat fluxes or null temperatures are prescribed at the top surface (see Fig. 10). Then, the solid flat layer is bounded by two semi-infinite solid media (see Fig. 11). The thermal material proper-

ties used are listed in the Tab. 1.

Table 1 : Thermal material properties

	Solid layer (concrete)	Lower solid medium (steel)	Top solid medium (steel)
Thermal conductivity ($W.m^{-1}.^{o}C^{-1}$)	$k_1 = 1.4$	$k_2 = 63.9$	$k_0 = 63.9$
Density ($Kg.m^{-3}$)	$\rho_1 = 2300$	$\rho_2 = 7832$	$\rho_0 = 7832$
Specific heat ($J.Kg^{-1}.^{o}C^{-1}$)	$c_1 = 880.0$	$c_2 = 434.0$	$c_0 = 434.0$

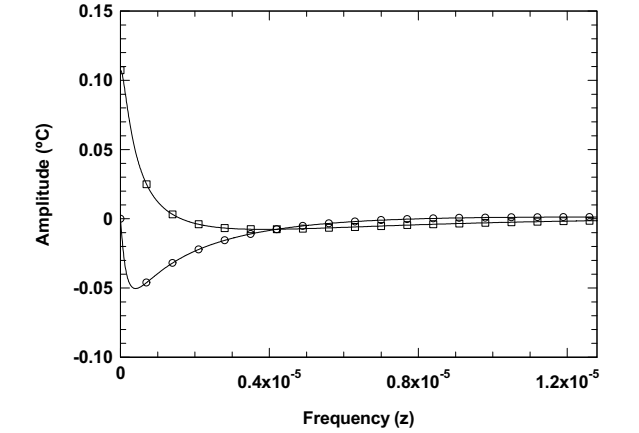

a)

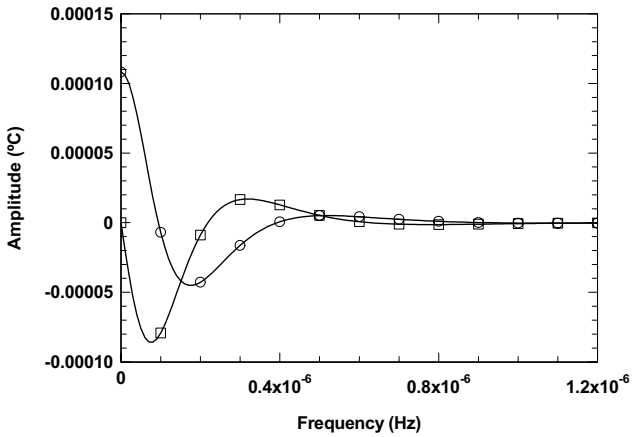

b)

Figure 11 : Solid layer bounded by two semi-infinite solid media: a) Receiver 1. b) Receiver 2

The three solid structures are heated by a harmonic point source applied in the solid layer medium at point ($x = 0.0\,\mathrm{m}, y = 1.2\,\mathrm{m}$). The computations are performed in the frequency range ($0{,}128 \times 10^{-7}\,\mathrm{Hz}$), with a frequency increment of $\Delta\omega = 1 \times 10^{-7}\,\mathrm{Hz}$. The imaginary part of the frequency has been set to $\eta = 0.7\Delta\omega$. To validate the results, the response is computed at a single value of $k_z (k_z = 0.4\,\mathrm{rad/m})$. The real and imaginary parts of the responses at receiver 1 ($x = 0.1\,\mathrm{m}, y = 0.75\,\mathrm{m}$) and receiver 2 ($x = 0.1\,\mathrm{m}, y = 5.75\,\mathrm{m}$) are shown in Fig. 10 and 11. The analytical responses are represented by the solid lines, while the marked points correspond to the BEM solution. The square and the round marks indicate the real and imaginary parts of the responses, respectively.

As can be seen, these two solutions are in very close agreement, and equally good results were obtained from tests in which sources and receivers were situated at different points.

6 Summary of Green's Functions

The Tables 2 – 5 summarizes the Green's functions presented throughout the paper.

Table 2 : Green's Functions in an Unbounded Medium.

Model	Equations
Three-dimensional	(3)
Two-dimenisonal ($k_z = 0$)	(5)
One-dimensioanl ($k_z = 0$, $k_{xn} = 0$)	(8)

Table 3 : Green's Functions in a Half-space

Boundary Conditions	Equations
Null normal flux at $y = 0$	(15)
Null temperature at $y = 0$,	(16)

7 Conclusions

The analytical solutions described here for calculating the heat propagation in unbounded, half-space, slab and layered media, when subjected to a spatially sinusoidal harmonic heat line source, appeared to be eminently suitable for performing transient heat conduction analyses.

Table 4 : Green's Functions in a Slab

Boundary Conditions	Equations
Null heat fluxes at the top and bottom surfaces	(18, 21), (22)
Null temperatures at the top surface and null heat fluxes at the bottom surface	(19, 21) , (23)
Null temperatures at the top and bottom surfaces	(20, 21) , (24)

Table 5 : Green's Functions in a Layered formation

Boundary Conditions	Equations
Solid layer over a solid half-space - null heat fluxes at $y = 0$.	(28, 30, 31)
Solid layer over a solid half-space - null temperatures at $y = 0$.	(29, 30, 31)
Solid layer bounded by two semi-infinite solid media.	(33, 34)
Multi-solid layer.	(39, 40)

In addition to the frequency responses, synthetic signatures were computed by means of inverse Fourier transformations, using complex frequencies in order to avoid the aliasing phenomenon.

The solutions presented were found to be in very close agreement with other analytical solutions in the case of unbounded, half-space and slab media and with the Boundary Elements Solution in the case of layered media, which requires the discretization of the solid interfaces with a large number of boundary elements.

The analytical solutions presented in this paper are intrinsically interesting. If the solutions are applied in conjunction with numerical methods, such as the BEM, they may prove to be very useful in many engineering applications, such as the calculation of the thermal insulation provided by solid walls and slabs.

References:

Bouchon, M. (1979): Discrete wave number representation of elastic wave fields in three-space dimensions. *Journal of Geophysical Research*, Vol. 84, pp. 3609-3614.

Bouchon, M.; Aki, K. (1977a): Time-domain transient Elastodynamic Analysis of 3D Solids by BEM. *Int. J. Numer. Methods in Eng.*, vol. 26, pp. 1709-1728.

Bouchon, M.; Aki, K. (1977b): Discrete wave-number representation of seismic-source wave field. *Bulletin of the Seismological Society of America*, vol. 67, pp. 259-277.

Carslaw, H. S.; Jaeger, J. C. (1959): Conduction of Heat in Solids, second edition. Oxford University Press.

Godinho, L.; António, J.; Tadeu, A. (2001): 3D sound scattering by rigid barriers in the vicinity of tall buildings. *Journal of Applied Acoustics*, vol. 62, n^o 11, pp. 1229-1248.

Kögl, M.; Gaul, L. (2000): A 3-D Boundary Element Method for Dynamic Analysis of Anisotropic Elastic Solids. *CMES: Computer Modeling in Engineering & Sciences*, Vol. 1, no 4, pp. 27-44.

Lamb, H. (1904): On the propagation of tremors at the surface of an elastic solid. *Phil. Trans. Roy. Soc. London*, A203:1-42.

Luco, J. E.; De Barros, F. C. P. (1995): Three-dimensional response of a layered cylindrical valley embedded in a layered half-space. *Earthquake Eng. Struct. Dyn.*, vol. 24, n^{o}1, pp. 109-125.

Manolis G. D.; Pavlou, S. (2002): A Green's Function for Variable Density Elastodynamics under Plane Strain Conditions by Hormander's Method. *CMES: Computer Modeling in Engineering & Sciences*, Vol. 3, no 3, pp. 399-416.

Ochiai, Y. (2001): Steady Steady Heat Conduction Analysis in Orthotropic Bodies by Triple-reciprocity BEM. *CMES: Computer Modeling in Engineering & Sciences*, Vol. 2, no 4, pp. 435-446.

Phinney, R. A. (1965): Theoretical calculation of the spectrum of first arrivals in the layered elastic medium. *J. Geophysics, Res.*, vol. 70, pp. 5107-5123.

Sellountos, E. J.; Polyzos, D. (2003): A MLPG (LBIE) Method for Solving Frequency Domain Elastic Problems. *CMES: Computer Modeling in Engineering & Sciences*, vol. 4, no. 6, pp. 619-636.

Stamos, A. A.; Beskos, D. E. (1996): 3-D seismic response analysis of long lined tunnels in half-space. *Soil Dyn. Earthquake Eng.*, vol. 15, pp. 111-118.

Stehfest, H. (1970): Algorithm 368: Numerical Inversion of Laplace Transform. *Communications of the Association for Computing Machinery*, vol. 13, n^o. 1, pp. 47-49.

Tadeu, A.; António, J. (2001): 2.5D Green's Functions for Elastodynamic Problems in Layered Acoustic and Elastic Formations. *CMES: Computer Modeling in Engineering & Sciences*, vol. 2, no 4, pp. 477-495.

Tadeu, A.; Godinho, L.; Santos, P. (2002): Wave motion between two fluid filled boreholes in an elastic medium. *Engineering Analysis with Boundary Elements*, EABE, vol. 26, n^o 2, pp. 101-117.

Tadeu, A.; Kausel, E. (2000): Green's functions for two-and-a-half dimensional elastodynamic problems. Journal of Engineering Mechanics - ASCE, vol. 126, n^o 10, pp. 1093-1097.

Zhang, L.; Chopra, A. K. (1991a): Three-dimensional analysis of spatially varying ground motions around a uniform canyon in a homogeneous half-space. *Earthquake Eng. Struct. Dyn.*, vol. 20, n^o 10, pp. 911-926.

Zhang, L.; Chopra, A. K. (1991b): Impedance functions for three-dimensional foundations supported on an infinitely-long canyon of uniform cross-section in a homogeneous half-space. *Earthquake Eng. Struct. Dyn.*, vol. 20, no 11, pp. 1011-1027.

Zhang, Ch.; Savaidis, A. (2003): 3-D Transient Dynamic Crack Analysis by a Novel Time-Domain BEM. *CMES: Computer Modeling in Engineering & Sciences*, vol. 4, no. 5, pp. 603-618.